

BROADBAND COMPLEX PERMITTIVITY MEASUREMENT OF LOW LOSS MATERIALS OVER LARGE TEMPERATURE RANGES BY STRIPLINE RESONATOR CAVITY USING SEGMENTATION CALCULATION METHOD

Y. Zhou, E. Li, G. Guo, Y. Gao, and T. Yang

School of Electronic Engineering
University of Electronic Science and Technology of China
Chengdu, Sichuan 611731, China

Abstract—A system has been developed for measuring the complex permittivity of low loss materials at frequencies from 500 MHz to 7 GHz and over a temperature range up to 1500°C using stripline resonator cavity method. Details of the design and fabrication of the cavity were discussed. Particular features related to high-temperature operation were described. An improved resonance method at high temperature for determining complex dielectric properties of low-loss materials was developed. The calculation process was given by a physical model of the stripline resonator cavity at high temperature. The paper brought forward the method of segmentation calculation according to the temperature changes over the cavity, which matched the actual situation of high temperature measurements. We have verified the proposed method from measurements of some typical samples with the available reference data in the literature.

1. INTRODUCTION

Complex permittivity is one of the most important parameters of microwave dielectrics. When the dielectrics work in high temperature environments, just as designing high-power devices and antenna windows, it is important to measure the dielectric properties of materials as a function of temperature. In recent years, many researchers have studied the high temperature measurements of the

dielectric properties of materials. The main test method is circular cavity resonance method, waveguide transmission/reflection method, open-ended coaxial probe method, and so on. Transmission/reflection method is commonly preferred to measure electromagnetic properties of microwave materials [1,2], and the temperatures can be up to 1000°C [3]. Open-ended coaxial probe method is usually used to measure complex permittivity at high temperatures due to the advantages of broad frequency band and simple measurement process [4–6]. But while applied in measuring low-loss materials these methods have high measurement uncertainties.

Cavity perturbation method is reported to measure complex permittivity at temperatures as high as 2000°C [7]. Circular cavity method has been generally used to measure complex permittivity of low-loss materials due to its relatively low measurement error margin. The method has been applied to high temperature measurement at microwave band at the temperatures 1200°C [8] and 1500°C [9]. Resonant methods have much better accuracy and sensitivity than nonresonant methods, they are generally applied to characterization of low-loss materials, the measurement accuracy of circular cavity resonance method is very high, but the physical size of the circular cavity at lower microwave frequencies is too large and very difficult to realize for high temperature measurements.

The stripline resonator cavity is much smaller than circular cavity over lower microwave frequency band. So this method is generally applied to the measurements of complex permittivity and permeability of low-loss materials at low microwave frequencies. Furthermore, the cavity is capable of multifrequency operation over a wide frequency range by using harmonics of the unit's fundamental resonance. Also, the sample is easy to fabricate and can be inserted through the open side of the resonator without otherwise disturbing the apparatus. Therefore, stripline resonator cavity was considered to measure the dielectric property at high temperatures in this paper. The cavity is illustrated in Figure 1, which is composed of two ground boards, one center conductor strip, and two end plates.

This method was first reported by Waldron [10,11] and Maxwell [12,13], improved by Musal [14] and Jones [15,16], and their works were carried out at room temperature. In this paper, we developed the measurement theory by considering the thermal expansion coefficient and the conductivity of the cavity metal as a function of temperature, a test system for measuring the complex permittivity of low-loss dielectrics at high temperatures was build. The test cavity used in this paper can work in temperature up to 1500 °C and cover the frequency band 500 MHz to 7 GHz.

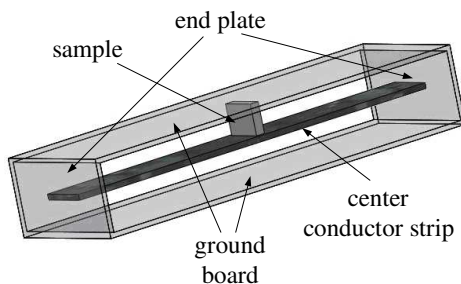


Figure 1. Stripline resonator cavity loaded with sample.

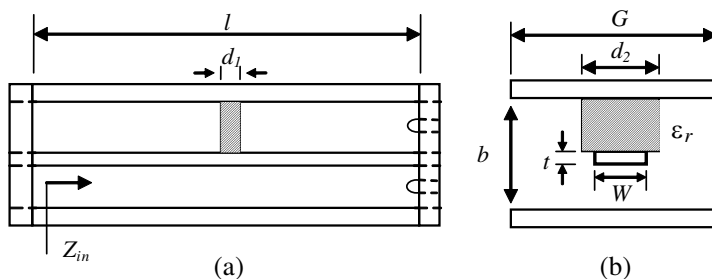


Figure 2. Structure of stripline resonator cavity.

The paper is organized as follows: Firstly, the stripline resonator and measurement theory at room temperature and high temperature are introduced in detail in Section 2 and Section 3 respectively. Section 4 introduced the cavity design. Section 5 presented the experimental apparatus and measurement setup. The measurement results and a discussion of the obtainable measurement accuracy are given in Section 6. The paper is then summarized in Section 7.

2. PHYSICAL MODEL AND THEORETICAL ANALYSIS AT ROOM TEMPERATURE

The structure and the cross section of the stripline resonator cavity are shown in Figure 2. l is the length of the cavity; G is the width of the ground board; b is the distance between the two ground boards; t and W are the thickness and width of the center conductor strip respectively.

We can use the formulas of literature [17] to calculate the characteristic impedance (Z_0) of stripline. The attenuation constant

(α_c) can be obtained by using the Wheeler's incremental inductance rule:

$$\alpha_c = \frac{2.7 \times 10^{-3} R_s \varepsilon_r Z_0}{30\pi (b-t)} A \quad \sqrt{\varepsilon_r} Z_0 < 120 \Omega \quad (1)$$

$$A = 1 + \frac{2W}{b-t} + \frac{1}{\pi} \frac{b+t}{b-t} \ln \left(\frac{2b-t}{t} \right) \quad (2)$$

$$R_s = \sqrt{\omega \mu_0 / 2\sigma_0} \quad (3)$$

where σ_0 is the conductivity of the conductors at room temperature, and μ_0 is free space permeability. The input impedance of the stripline resonator cavity is:

$$Z_{in} = Z_0 \frac{Z_L + Z_0 \tanh(\gamma l)}{Z_0 + Z_L \tanh(\gamma l)} \quad (4)$$

where

$$\gamma = \alpha + j\beta \quad (5)$$

$$\beta = 2\pi/\lambda = \omega/c \quad (6)$$

The stripline cavity is air-filled, so $\alpha = \alpha_c$. When the stripline is terminated by end plate, $Z_L = 0$, we derived the following expressions for the input impedance:

$$\begin{aligned} Z_{in} &= Z_0 \tanh(\alpha + j\beta) l = Z_0 \frac{\tanh(\alpha l) + j \tan(\beta l)}{1 + j \tan(\beta l) \tanh(\alpha l)} \\ &= Z_0 \frac{\tanh(\alpha l) + \tan^2(\beta l) \tanh(\alpha l)}{1 + \tan^2(\beta l) \tanh^2(\alpha l)} + j Z_0 \frac{\tan(\beta l) [1 - \tanh^2(\alpha l)]}{1 + \tan^2(\beta l) \tanh^2(\alpha l)} \\ &= R + jX \end{aligned} \quad (7)$$

According to the resonance condition, $X = 0$, that means $\tan(\beta l) = 0$. The resonant length can be calculated as $l = n\lambda/2$, $n = 1, 2, 3 \dots$. The cavity length could be amended by measuring the resonant frequency at room temperature. We have $R = Z_0 \tanh(\alpha l)$ at the resonant frequency. The attenuation constant α_c is related to the measured quality factor (Q) as $\alpha_c = n\pi/2Ql$. We can obtain σ_0 through Equations (1) to (3).

After sample is loaded in the center of the cavity, the resonant frequency and quality factor changed. Figure 2(b) shows the cross section of the test device. Because of the heterogeneity of the cross section, TEM wave cannot be propagated. However, for low frequencies, longitudinal components of the microwave fields can be neglected compared with transversal ones. So, the hypothesis of a quasi-TEM mode is valid, the validity domain of this approximation

is justified in the centimeter wave band. The quasistatic theory has been used to determine the characteristic impedance (Z_{01}) and the propagation constant (γ_1) of the stripline, the relationship between the complex permittivity (ϵ_r and $\tan\delta$) of the sample and the propagation constant can be determined. This approach, based on the Green's potential functions and on the transverse transmission line method [18]. Under these assumptions, the input impedance of the stripline resonator cavity is:

$$Z_{in} = Z_0 \frac{Z_{L1} + Z_0 \tanh \left[\frac{\gamma(l - d_1)}{2} \right]}{Z_0 + Z_{L1} \tanh \left[\frac{\gamma(l - d_1)}{2} \right]} = R_1 + jX_1 \quad (8)$$

where

$$Z_{L1} = Z_{01} \frac{Z_{L2} + Z_{01} \tanh(\gamma_1 d_1)}{Z_{01} + Z_{L2} \tanh(\gamma_1 d_1)} \quad (9)$$

$$Z_{L2} = Z_0 \tanh \left[\frac{\gamma(l - d_1)}{2} \right] \quad (10)$$

the resonance condition is $X_1 = 0$, the quality factor is:

$$Q = \frac{\omega_0}{2R_1} \left. \frac{\partial X_1}{\partial \omega} \right|_{\omega=\omega_0} \quad (11)$$

d_1 is the thickness of the sample. The complex permittivity of the sample can be calculated by computer from the measured resonant frequency and quality factor of the sample loaded cavity.

3. ANALYSIS AT HIGH TEMPERATURES

When the stripline resonator cavity was applied to measure dielectric property at high temperatures, we put the whole cavity into a vacuum furnace to avoid oxidation, but the cavity was connected to the test equipments outside the furnace. In this case, it is impossible to keep the whole cavity at the same high temperature. In practice, only the sample region of the cavity needs to be heated to the test temperature, so the temperature is different in the direction along the cavity length. The main difference between the measurements at room temperature and at variable temperatures is that the thermal expansion coefficient and conductivity of the cavity metal is variable and dependent on the temperature. We use the new method of segmentation calculation to analyze the resonant frequency and quality factor considering the temperature differences along the stripline resonator cavity. We also

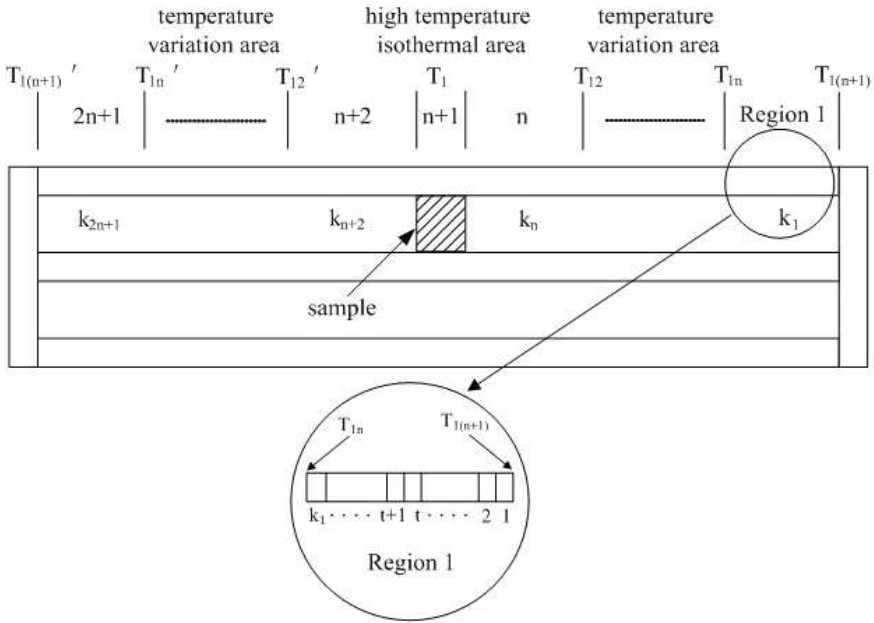


Figure 3. Physical model of the cavity at high temperature.

consider that the cross section dimension of the stripline cavity varies and the conductivity changes with different temperatures.

Complex permittivity measurements were performed by placing the sample at the axial midpoint of the center conductor strip. Therefore, only the midpoint of the cavity needs to be heated to the test temperature. The physical model is illustrated in Figure 3.

First we have to calibrate the empty cavity at each test temperature. The cavity was divided into $2n + 1$ segments, and the midpoint of the cavity is in the high temperature isothermal area. Temperature variation areas on both sides were divided into n segments. Temperatures were measured with thermocouples buried in the ground boards of the cavity. Figure 3 shows the temperature gradient when the temperature rises from room temperature T_0 to the first test temperature T_1 . The temperature of the right end of temperature region 1 measured by thermocouple is defined as $T_{1(n+1)}$. The measured temperature next to $T_{1(n+1)}$ is defined as T_{1n} , region 1 is divided into k_1 parts, then the temperature of each part can be obtained by linear interpolation.

$T_{11}(t)$ means the temperature of part t of region 1. The first subscript represents the first test temperature; the second subscript

represents the number of the temperature region; t represents the t part of the temperature region.

$$T_{11}(t) = T_{1(n+1)} + \frac{T_{1n} - T_{1(n+1)}}{k_1} \times \left(t - \frac{1}{2}\right) \quad 1 \leq t \leq k_1 \quad (12)$$

The temperature of region n , part t is:

$$T_{1n}(t) = T_{12} + \frac{T_1 - T_{12}}{k_n} \times \left(t - \frac{1}{2}\right) \quad 1 \leq t \leq k_n \quad (13)$$

The temperature of region $2n + 1$, part t is:

$$T_{1(2n+1)}(t) = T'_{1n} + \frac{T'_{1(n+1)} - T'_{1n}}{k_{2n+1}} \times \left(t - \frac{1}{2}\right) \quad 1 \leq t \leq k_{2n+1} \quad (14)$$

If there is little difference between T_0 and T_1 , the linear thermal expansion coefficient of the metal material used to fabricate the cavity can be approximately regarded as stable. The characteristic impedance of stripline will not change due to linear thermal expansion of all directions in the cross section are equal.

The linear thermal expansion coefficient of the cavity material is denoted as Δ_1 at temperatures between T_0 and T_1 , so the length of region m ($1 \leq m \leq 2n + 1$), part t is:

$$l_{1m}(t) = \frac{l_{0m}}{k_m} (1 + \Delta_1 \times (T_{1m}(t) - T_0)) \quad 1 \leq t \leq k_m \quad (15)$$

l_{0m} means the length of region m at room temperature T , the length of region m is:

$$l_{1m} = \sum_{t=1}^{k_m} l_{1m}(t) = \sum_{t=1}^{k_m} \left(\frac{l_{0m}}{k_m} (1 + \Delta_1 \times (T_{1m}(t) - T_0)) \right) \quad (16)$$

The total length of the cavity after it is heated to the first temperature is:

$$l_1 = \sum_{m=1}^{2n+1} l_{1m} = \sum_{m=1}^{2n+1} \sum_{t=1}^{k_m} l_{1m}(t) = \sum_{m=1}^{2n+1} \sum_{t=1}^{k_m} \left(\frac{l_{0m}}{k_m} (1 + \Delta_1 \times (T_{1m}(t) - T_0)) \right) \quad (17)$$

It is assumed that the conductivity of the cavity metal is linearly dependent on temperatures between T_0 and T_1 , the change rate of conductivity is recorded as $\Delta\sigma_1$. So the conductivity of region m , part t can be expressed as:

$$\sigma_{1m}(t) = \sigma_0 + \Delta\sigma_1 \times (T_{1m}(t) - T_0) \quad 1 \leq t \leq k_m \quad (18)$$

The attenuation constant can be derived by Equation (1). b and t can be calculated using the Δ_1 and the geometrical measurement of

the cavity at room temperature. Then, the propagation constant of each part can be calculated.

The following is the calculation process of the resonant frequency and the quality factor according to the attenuation constant and the dimension of each temperature region. The input impedance of part 1 in region 1 is:

$$Z_{11}(l_{11}(1)) = Z_0 \frac{Z_L + Z_0 \tanh[\gamma_{11}(1)l_{11}(1)]}{Z_0 + Z_L \tanh[\gamma_{11}(1)l_{11}(1)]} \quad (19)$$

where $Z_L = 0$. The input impedance of part t in region m is:

$$Z_{1m}(l_{1m}(t)) = Z_0 \frac{Z_{1m}(l_{1m}(t-1)) + Z_0 \tanh[\gamma_{1m}(t)l_{1m}(t)]}{Z_0 + Z_{1m}(l_{1m}(t-1)) \tanh[\gamma_{1m}(t)l_{1m}(t)]} \quad (20)$$

The input impedance of next part can be obtained by the input impedance of precious parts, etc., the total input impedance is:

$$\begin{aligned} Z_{total} &= Z_{1(2n+1)}(l_{1(2n+1)}(k_{2n+1})) \\ &= Z_0 \frac{Z_{1(2n+1)}(l_{1(2n+1)}(k_{2n+1}-1)) + Z_0 \tanh[\gamma_{1(2n+1)}(k_{2n+1})l_{1(2n+1)}(k_{2n+1})]}{Z_0 + Z_{1(2n+1)}(l_{1(2n+1)}(k_{2n+1}-1)) \tanh[\gamma_{1(2n+1)}(k_{2n+1})l_{1(2n+1)}(k_{2n+1})]} \\ &= R_m + jX_m \end{aligned} \quad (21)$$

Based on the resonance condition $X_m = 0$, we have:

$$\tan\left(\beta \sum_{m=1}^{2n+1} \sum_{t=1}^{k_m} l_{1m}(t)\right) = \tan(\beta l_1) = 0 \quad (22)$$

So $l_1 = n\lambda/2 = nc/2f$, $n = 1, 2, 3 \dots$

The resonant frequency is only related with the total length of the cavity. So the total length of the cavity at test temperature can be obtained by the measured resonant frequency. Then Δ_1 can be calculated from Equation (17). Equation (15) gives the length of each part at variable temperatures, where l_{0m} can be calculated through the measured resonant frequency at room temperature.

The quality factor is:

$$Q = \frac{\omega_0}{2R_m} \left. \frac{\partial X_m}{\partial \omega} \right|_{\omega=\omega_0} \quad (23)$$

$\Delta\sigma_1$ can be derived through measured quality factor, and then we get the conductivity of each segment from Equation (18). The first calibration at temperature T_1 has been finished. The second step is heating the cavity to temperature T_2 and then calculating the temperature of each part by measured temperature. When the temperature of any part of the cavity is between T_0 and T_1 , the metal linear expansion coefficient and conductivity of this part could use the

value obtained by step 1. When the temperature is between T_1 and T_2 , the conductivity change rate was recorded as $\Delta\sigma_2$, and cavity metal linear expansion coefficient was recorded as Δ_2 . We can get the $\Delta\sigma_2$ and Δ_2 through the measured resonant frequency and quality factor following the scheme provided above.

We gradually increase the cavity temperature and record the frequency and quality factor at every test temperature. Using the parameters at previous temperatures and the measured resonant frequency and quality factor at current temperature, the conductivity change rate and cavity metal linear expansion coefficient at each temperature section can be derived. Finally the calibration of the cavity at variable temperatures could be done according to these steps.

After sample is loaded in the center of the cavity, the resonance frequencies of loaded cavity depend both on the thermal expansion coefficient of the metal cavity and the relative dielectric constant of the dielectric interior. We heated the loaded cavity to the same temperature as the empty cavity, and the resonant frequencies and quality factors of the different modes of the loaded cavity are obtained. Dielectric constant and loss tangent at various temperatures and frequencies can be determined by applied segmentation calculation method to Equations (8) and (11). The thermal expansion coefficient and conductivity of each segment are determined according to the temperature distribution of the loaded cavity. The process of the measurement is automated by the computer.

From all the steps discussed above, the measurement process can be summarized as follows: (1) resonant frequencies and quality factors in the empty cavity as function of temperature are measured; (2) conductivity and thermal expansion constant of the cavity metal as function of temperature are calculated; (3) resonant frequencies and quality factors as function of temperature with the sample inside the cavity are measured; (4) finally, loss tangent and permittivity are computed as function of temperature from the measured and calculated data, using standard procedures based on segmentation calculation method which described in detail beforehand.

4. CAVITY DESIGN

The stripline resonator cavity was operated in the TE_{00n} mode. Higher-order modes (i.e., TM_{mn} and $TM_{m'n'}$ modes) were found to overlap with other nearby, densely spaced modes, rendering it difficult to clearly ascertain their resonance lineshape properties (Figure 4(a)). The dimensions of the cavity must be carefully designed to reduce the number of the disturbing modes or make the disturbing modes away

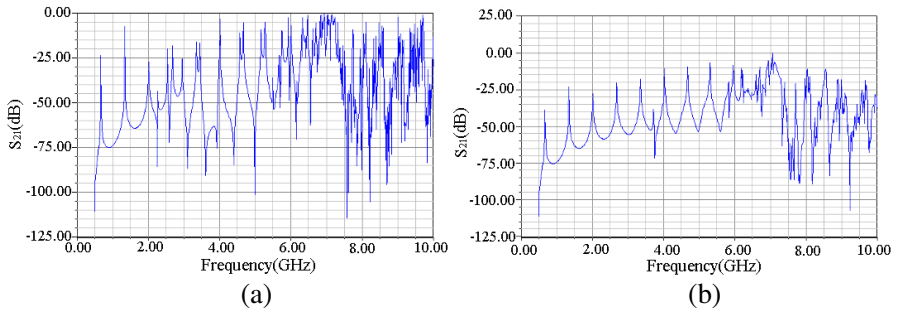


Figure 4. Simulation result of the cavity. (a) Before optimization. (b) After optimization.

from the working modes as far as possible, Otherwise, the dimensions of the cavity must be optimized to achieve high quality factor.

In this work, we have performed sensitivity analysis in an effort to find the optimum stripline aperture dimensions (t , W , b , G) to obtain both the high quality factor and easy to distinguish working modes. The physical size of the cavity was obtained after optimization and simulation. Figure 4(b) shows the simulation result of the optimized cavity. The designed cavity has “clear” resonant modes and high quality factors, which assures the accurate measurement of complex permittivity on the basis of theory.

A propagating TEM mode is excited within the stripline structure using either coupling loops mounted in one of the end plates or two coupling loops distributed symmetrically in the ground plane near the both sides of the two end planes and adjustable in axial position. The fundamental resonance is achieved when the cavity length corresponds to a half-guide wavelength of the exciting frequency. Additional resonances will occur at harmonic frequencies of the fundamental.

Since the test cavity would work in temperature as high as 1500°C , the selection of the metal used to fabricate the cavity was very important. The cavity metal should have excellent conductivity to ensure that the cavity can still resonate at high temperature. Ordinary metal could not meet the requirement. After careful study and cost consideration, metal molybdenum was selected as the metal to fabricate the cavity. Metal molybdenum has high conductance at high temperatures and can be fabricated easily, but has the disadvantage to be easily oxidized when exposed in air atmosphere. In order to solve this problem, vacuum furnace is applied to heat the sample and cavity and the surface of the cavity was coated with metal iridium which is stable at high temperature (Figure 5).



Figure 5. Photograph of the stripline resonator cavity.

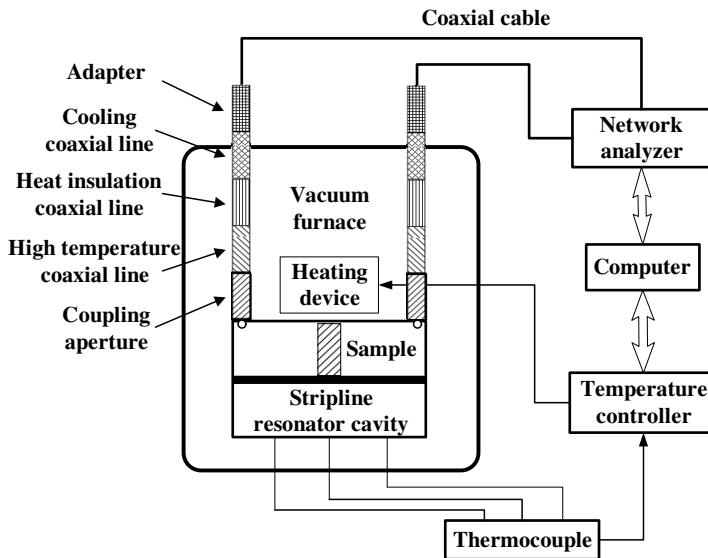


Figure 6. Block diagram of high temperature test system.

5. TEST SYSTEM

The test system for temperature dependence of complex permittivity consists of network analyzer, computer, temperature control instrument, coupling aperture, high temperature coaxial line, heat insulation coaxial line, cooling coaxial line, adapters and vacuum furnace as shown in Figure 6. In order to heat the sample region up to 1500°C , a resistive heating ring was fixed at the center of the cavity. Adapters are used to connect coaxial cables with cooling coaxial lines which are cooled by water to ensure the adapters and coaxial cables work in room temperature. The wall of the heat insulation coaxial line is thin to prevent significant thermal conduction from the hot cavity to the cooling coaxial line. Each coupling aperture is connected with a



Figure 7. Photograph of the test system.

high temperature coaxial line which is made of metal molybdenum. Temperatures are measured with thermocouples buried in the ground boards of the cavity. Computer controls temperature via the temperature controller by reading the thermocouple and varying the current to heat the cavity. Figure 7 is the photograph of the test system.

At first, heat the empty cavity at different temperatures. When the temperature reaches a test temperature, wait for few minutes then measure the resonant frequencies and quality factors of different working modes. After the test system is cooled to room temperature, the sample is loaded into the cavity. When the temperature reaches the same temperature as the empty cavity, wait for few minutes to heat the sample region to the same temperature, then measure the resonant frequencies and quality factors of the loaded cavity. The resonant frequencies and quality factors can be automatically measured by network analyzer and be transmitted into computer through GPIB card. And the complex permittivity of microwave dielectric substrate can be calculated at the same time by test software. All of the measurement process is automated by computer.

6. MEASUREMENT RESULTS

The repeated measurement results of resonant frequencies and unloaded quality factors of some typical resonant modes are shown in Figures 8–11, respectively. The repeatability of frequencies is less than 1 MHz and the quality factors less than 20. The good repeatability of the empty cavity ensures the accurate measurement of the dielectric properties.

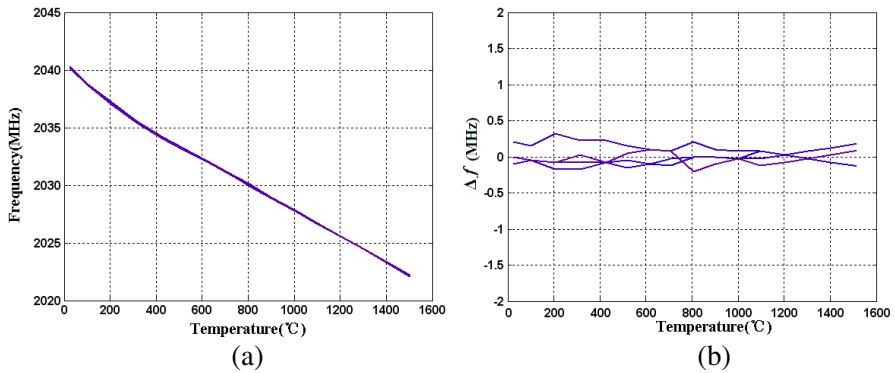


Figure 8. Repeated measurements of the resonant frequency of TEM₀₀₃ mode. (a) Resonant frequencies versus temperature. (b) The variation of resonant frequencies.

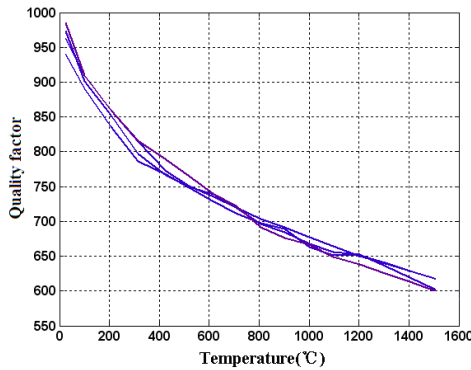


Figure 9. Repeated measurements of the quality factor of TEM₀₀₃ mode.

To illustrate the capabilities of this hardware system developed in the paper, we have measured the complex permittivity of homogeneous and isotropic fused quartz. Figures 12 and 13 show the measurement results of the dielectric constant and the loss tangent of the sample dependent on temperature of each resonant frequency, respectively. Tables 1 and 2 list the measured values for three quartz samples made of same material. The measurement results show the high repeatability of the test system. Note that the measured dielectric constants are in excellent agreement with the ones from MIT and CRC, and the results of loss tangent are between the ones from MIT and CRC at

Table 1. Measurement results of permittivity of quartz samples at 7358 MHz and data from MIT and CRC.

Temperature (°C)	Data using the system in this paper			MIT Data (8.52 GHz)	CRC Data (9.4 GHz)
25	3.830	3.828	3.829	3.82	3.81
100	3.831	3.830	3.830	3.83	/
200	3.835	3.833	3.834	3.84	3.83
300	3.845	3.842	3.841	3.84	/
400	3.851	3.849	3.850	3.86	3.84
500	3.862	3.860	3.862	3.87	/
600	3.870	3.868	3.869	3.88	3.86
700	3.885	3.880	3.884	3.89	/
800	3.898	3.892	3.900	3.90	3.88
900	3.904	3.901	3.903	3.91	/
1000	3.912	3.909	3.911	/	3.91
1100	3.923	3.919	3.921	/	/
1200	3.935	3.930	3.936	/	3.93
1300	3.946	3.942	3.947	/	/
1400	3.958	3.960	3.962	/	3.96
1500	3.970	3.975	3.971	/	/

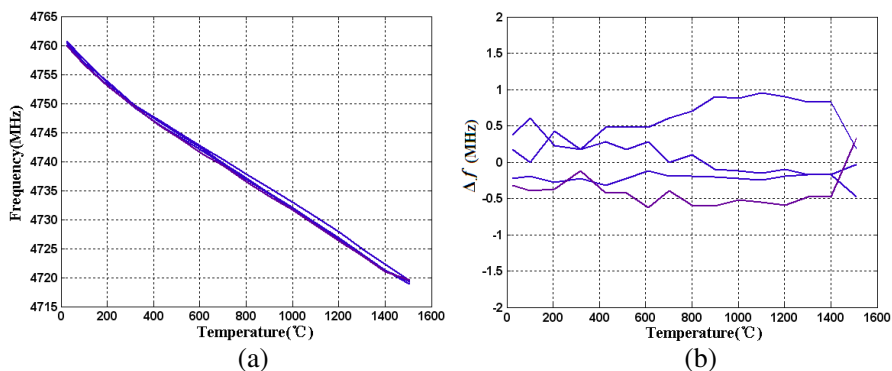


Figure 10. Repeated measurements of the resonant frequency of TEM_{007} mode. (a) Resonant frequencies versus temperature. (b) The variation of resonant frequencies.

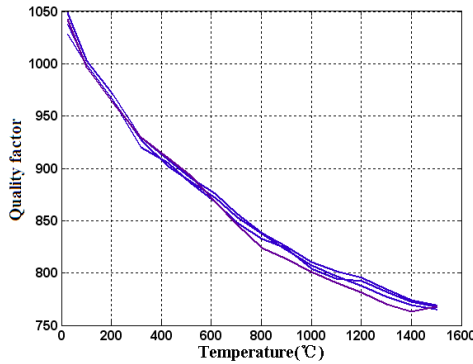


Figure 11. Repeated measurements of the quality factor of TEM₀₀₇ mode.

Table 2. Measurement results of loss tangent of quartz samples at 7358 MHz and data from MIT and CRC.

Temperature (°C)	Data using the system in this paper			MIT Data (8.52 GHz)	CRC Data (9.4 GHz)
25	0.000552	0.000550	0.000548	0.00015	0.00015
100	0.000556	0.000555	0.000553	0.00014	/
200	0.000567	0.000564	0.000569	0.00012	0.00018
300	0.000572	0.000571	0.000574	0.00012	/
400	0.000586	0.000581	0.000589	0.00012	0.0002
500	0.000592	0.000595	0.000599	0.00012	/
600	0.000605	0.000603	0.000605	0.00014	0.00029
700	0.000621	0.000625	0.000624	0.00014	/
800	0.000632	0.000630	0.000635	0.00014	0.00048
900	0.000650	0.000648	0.000651	0.00014	/
1000	0.000662	0.000665	0.000663	/	0.0011
1100	0.000683	0.000680	0.000690	/	/
1200	0.000701	0.000698	0.000709	/	0.0025
1300	0.000725	0.000720	0.000731	/	/
1400	0.000745	0.000738	0.000748	/	0.0046
1500	0.000762	0.000756	0.000766	/	/

high temperature [19]. MIT used circular cavity resonance method which has higher quality factor than stripline resonator cavity, so it has much better accuracy in determine loss tangent. CRC used short-circuited method which has higher measurement uncertainty for loss tangent when measuring low-loss materials at high temperature.

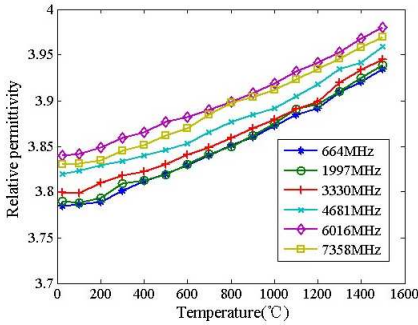


Figure 12. Temperature and frequency dependences of dielectric constant of quartz.

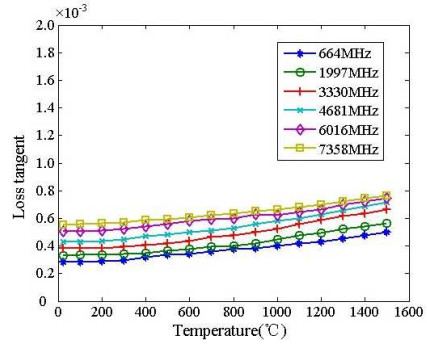


Figure 13. Temperature and frequency dependences of loss tangent of quartz.

For the setup described here, the measurement uncertainties are less than 2.5% in dielectric constant and 20% in loss tangent for room temperature measurements, and less than 4% in dielectric constant and 35% in loss tangent for high temperature measurements, respectively. The uncertainties given are analyzed and based on the measurement ranges of the system, which is excellent compared to other experimental techniques in the low microwave frequencies at high temperature. Compared with the MIT and CRC data, the loss tangent differences are caused by different samples with different impurity and measurement uncertainties.

7. CONCLUSION

This paper presents a broad-band technique for measuring the complex permittivity of low loss material over wide temperature ranges at low microwave frequencies. We described the design and performance of the test system. The thermal expansion and the conductivity for cavity metal have been calculated as a function of temperature based on the measured data of the empty cavity. We establish the physical model at variable temperature and propose the method of segmentation calculation according to the temperature changes along the cavity. The test system can provide reliable measurement results at temperatures from room temperature to 1500°C with the broad frequency range 500 MHz–7 GHz. The measurement uncertainties of the test system are 2.5% for dielectric constant and 20% for loss tangent at room temperatures, and 4% for dielectric constant and 35% for loss tangent at high temperatures respectively.

The shortcoming of the test system is that the quality factor of stripline cavity is low especially at high temperatures, so measurement uncertainty for loss tangent is high when measuring low-loss materials. The cavity metal should have excellent conductivity and work stable at high temperature. In future work, the metal should be carefully selected based on lots of experiments at high temperature. In addition, we believe the frequency of the test system can be expanded to other bands and elevated to higher temperature.

REFERENCES

1. Hasar, U. C., "Unique permittivity determination of low-loss dielectric materials from transmission measurements at microwave frequencies," *Progress In Electromagnetics Research*, Vol. 107, 31–46, 2010.
2. Hasar, U. C. and E. A. OralA, "Metric function for fast and accurate permittivity determination of low-to-high-loss materials from reflection measurements," *Progress In Electromagnetics Research*, Vol. 107, 394–412, 2010.
3. Hauschild, T. and R. K. Ochel, "Measurement of complex permittivity of solids up to 1000°C," *Microwave Symposium Digest*, 1687–1690, San Francisco, CA, USA, June 17–21, 1996.
4. Gershon, D. L., J. P. Calame, Y. Carmel, T. M. Antonsen, Jr., and R. M. Hutcheon, "Open-ended coaxial probe for high-temperature and broad-band dielectric measurements," *IEEE Transactions on Microwave Theory and Technology*, Vol. 56, No. 3, 684–692, 2008.
5. Ma, L. X., H. Zhang, and C. X. Zhang, "Analysis on the reflection characteristic of electromagnetic wave incidence in closed nonmagnetized plasma," *Journal of Electromagnetic Waves and Applications*, Vol. 22, No. 17–18, 2285–2296, 2008.
6. Wang, Z., W. Che, and L. Zhou., "Uncertainty analysis of the rational function model used in the complex permittivity measurement of biological tissues using PMCT probes within a wide microwave frequency band," *Progress In Electromagnetics Research*, Vol. 90, 137–150, 2009.
7. Baeraky, T. A., "Microwave measurements of dielectric properties of zinc oxide at high temperature," *Egyptian Journal of Solids*, Vol. 30, No. 1, 13–18, 2007.
8. Li, Y., J. Li, and X. He, "Study on high temperature dielectric properties of magnetic window materials by cavity resonator method," *Journal of Infrared and Millimeter Waves*, Vol. 23, No. 2, 157–160, April 2004.

9. Li, E., Z.-P. Nie, G. Guo, Q. Zhang, Z. Li, and F. He, "Broadband measurements of dielectric properties of low-loss materials at high temperatures using circular cavity method," *Progress In Electromagnetics Research*, Vol. 92, 103–120, 2009.
10. Waldron, R. A., "Theory of a strip-line cavity for measurement of dielectric constants and gyromagnetic-resonance line-widths," *IEEE Transactions on Microwave Theory and Technology*, Vol. 12, No. 1, 123–131, 1964.
11. Waldron, R. A., "Theory of the strip-line cavity resonator," *Marconi Rev.*, Vol. 27, 30–42, 1964.
12. Maxwell, S., "A stripline cavity resonator for measurement of ferrites," *Microwave J.*, Vol. 9, 99–102, 1966.
13. Maxwell, S., "Strip-line cavity resonator for measurement of magnetic and dielectric properties of ferrites at low microwave frequencies," *Marconi Rev.*, Vol. 27, 22–29, 1964.
14. Musal, H. M., "Demagnetization effect in strip-line cavity measurements," *IEEE Transactions on Magnetics*, Vol. 28, No. 5, 3129–3131, 1992.
15. Jones, C. A., "Permeability and permittivity measurements using stripline resonator cavities: A comparison," *IEEE Transactions on Instrumentation and Measurement*, Vol. 48, No. 4, 843–848, 1999.
16. Weil, C. M., C. A. Jones, Y. Kantur, and J. H. Grosvenor, Jr., "On RF material characterization in the stripline cavity," *IEEE Transactions on Microwave Theory and Techniques*, Vol. 48, No. 2, 266–275, 2000.
17. Wheeler, H. A., "Transmission-line properties of a strip line between parallel planes," *IEEE Transactions on Microwave Theory and Techniques*, Vol. 26, No. 11, 866–876, 1978.
18. Crampagne, R., M. Ahmadpanah, and J.-L. Guiraud, "A simple method for determining the Green's function for a large class of MIC lines having multilayered dielectric structures," *IEEE Transactions on Microwave Theory and Techniques*, Vol. 26, No. 2, 82–87, 1978.
19. Shackelford, J. F. and W. Alexander, *CRC Materials and Engineering Handbook*, CRC Press, 2001.